Dual-sensor summation with buried land sensors

Dmitry Alexandrov, Saint Petersburg State University; Andrey Bakulin, EXPEC Advanced Research Center, Saudi Aramco; Pierre Leger, Saudi Aramco; Boris Kashtan, Saint Petersburg State University*

Summary

Up-down wavefield separation is often performed with dual-sensor summation, where collocated hydrophone and geophone responses are summed after application of an appropriate scalar. While this technique can be used in both land and marine surveys, scalar selection can be more challenging for land applications since the receiver may be placed in heterogeneous media. Here we present a method for scalar estimation using buried receiver data. This approach utilizes the autocorrelation of a summed geophone and hydrophone. We show that the correct calibration scalar delivers minimum to this autocorrelation at specific locations. We develop an algorithm for estimation of this summation scalar and test it on a realistic horizontally layered media.

Introduction

Dual-sensor summation is a well-known technique used in marine or ocean-bottom seismic to perform up-down wavefield separation (Barr, 1997). This method can also be applied to land seismic surveys (Burnstad et al., 2012). Wavefield separation is achieved through summation of hydrophone records with scaled geophone records. In theory, for laterally invariant media with known parameters, scalars can be computed as the acoustic impedance of the layer where the sensors are placed Wapenaar (1998). In practice, scalars need to be estimated from the data itself because of many unknown parameters (Barr, 1997). Soubaras (1996) presented a data driven approach for geophone calibration in the frequency domain using a filter related to the receiver side ghost for ocean-bottom receivers. In this case we have a homogeneous water layer between receivers and the free surface generating ghost arrivals. Dragoset and Barr (1994) described an alternative method to derive geophone scalars from the field data in the time domain. Here we are using similar approach but for a completely general case when receivers are placed in a media with arbitrary layering, resulting in many additional boundaries between the receiver location and free surface. We are motivated by land acquisition with buried receivers (Bakulin et al., 2012) where dual-sensor summation showed good promise (Burnstad et al., 2012) but deriving the geophone scalar proved to be more challenging. For buried receivers, the initial value of the scalar can be derived from first breaks (early arrivals), based on the assumption that the initial phases represent mainly downward propagating waves. However, this assumption can be violated when receivers are located in the vicinity of high acoustic contrasts. In such circumstances, early arrivals will be influenced by upgoing energy. In order to refine this initial estimate, we present a new approach that relies on reflected energy from a deeper gate. We use cross-correlation of geophone and hydrophone records to estimate the time delay between reflection and ghost arrivals coming from the free surface. We then scale the geophone response with a trial scalar and compute the autocorrelation of the sum of geophone and hydrophone records. We demonstrate that with the correct calibration scalar, amplitudes of the autocorrelation trace are minimized at the two-way traveltime from the receiver to the free surface. Therefore, the task of finding a geophone scalar can be formulated as a minimization problem. We first explain the basics of this approach using a simple model with a single reflector and free surface. Then we describe the method in more detail and apply it to a realistic model with a large number of layers.

Method

To demonstrate the basics of this method, let us consider a simple elastic model with a single reflector at 1000 m and a free surface. A surface source generates elastic waves which are registered by the collocated geophone and hydrophone placed at 300 m depth (Figure 1a). The geophone measures vertical particle velocity while the pressure field detected by the hydrophone is simulated in elastic media by taking the divergence of the displacement field. The primary reflection and receiver ghost arrivals are shown in Figures 1b and 1c for the geophone and hydrophone respectively. Geophone (G) and hydrophone (H) measurements can be expressed in terms of upgoing (U) and downgoing (D) wavefields:

$$G_0 = U + D,\ H = U - D \tag{1}$$

Here, $G_0 = s_0 G$ is the scaled geophone data and s_0 is a calibration scalar. If the geophone is already scaled properly, then s_0 is equal to 1. Note that downgoing parts of the hydrophone and geophone have opposite signs. This is consistent with synthetic traces in Figures 1b and 1c.

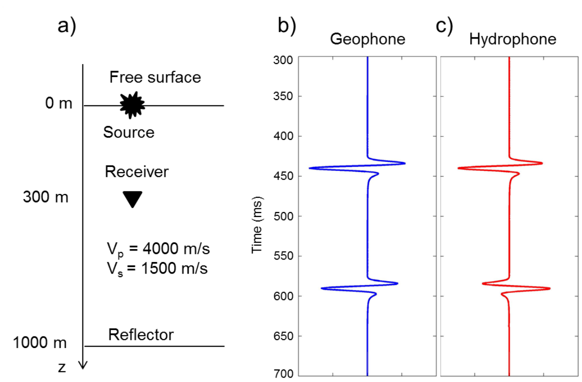

Figure 1: A sketch of the model with a single reflector (a), and reflection arrivals recorded by geophone (b) and hydrophone (c).

In our simple model, up-going waves will arrive from the reflector, whereas the downgoing wavefield will contain a direct wave and ghost reflections from the free surface. The part of

DOI http://dx.doi.org/10.1190/segam2014-1082.1

the downgoing wavefield without the direct wave can be obtained from the up-going wavefield with a propagator Z:

$$D = ZU \tag{2}$$

In this case, Z introduces some amplitude reduction due to geometrical spreading and a time delay equal to the two-way travel time ($2\Delta t$) from receiver level to the free surface:

$$Z(\omega)\, e^{-i\omega 2\Delta t},$$

where ω designates cyclic frequency.

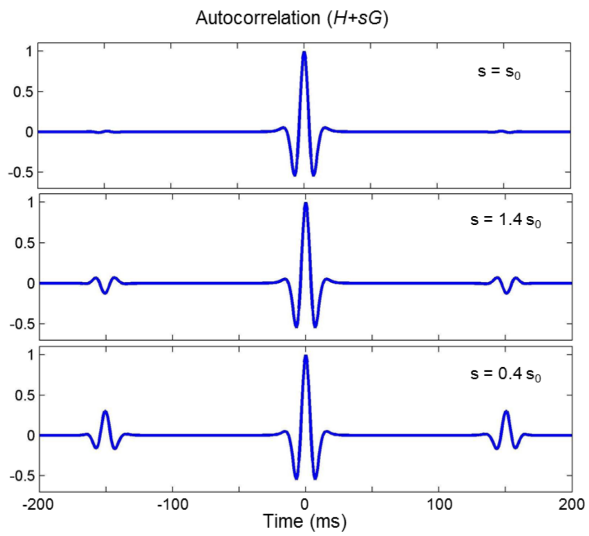

Figure 2: Autocorreltaion of summed hydrophone and scaled geophone zero-offset traces with correct calibration scalar $s = s_0$ (a), and with incorrect calibration $s = 1.4s_0$ (b) and $s = 0.4s_0$ (c).

Let us assume that we do not know the calibration scalar s_0. Consider the autocorrelation of the sum $H + sG$, where s is a parameter we can vary. From equations 1 and 2 it follows that in the frequency domain this autocorrelation is equal to

$$(H+sG)^*(H+sG) = \\ = \frac{U^*U}{s_0^2}\left\{(s+s_0)^2 + Z^*Z(s-s_0)^2 + (s^2 - s_0^2)(Z^* + Z)\right\} \tag{3}$$

Where * denotes the complex conjugate. In order to use equation refeqn:eq2 we mute direct arrivals on both geophone and hydrophone records before autocorrelation. In the time domain the first two summands of equation 3 give a signal at $t = 0$ ms. Note that Z^*Z does not introduce a time shift. The third summand creates peaks at $t = 2\Delta t$ and $t = -2\Delta t$. It is clear from equation 3 that if we choose s equal to the calibration scalar s_0, then there will be no peaks at $t = \pm 2\Delta t$ (Figure 2a). Therefore, the correct calibration scalar can be found by minimization of amplitude/energy inside the time window placed around $t = 2\Delta t$.

In some cases the exact value of the two-way travel time from sensor to the free surface may not be known or may require a more precise estimate. In complex media, with a large number of layers, ghost arrivals can be obscured with multiple reflections from other layers and may be hard to identify. The cross-correlation of the geophone and hydrophone records can be used to determine Δt in such cases:

$$G^*H \sim U^*U(1 - Z^*Z) + U^*UZ^* - U^*UZ \tag{4}$$

Regardless of whether the geophone is calibrated or not, summands U^*UZ^* and $-U^*UZ$ create antisymmetric events in the time domain at $t = \pm 2\Delta t$ (Figure 3). The autocorrelation 3 contains symmetric events at $t = \pm 2\Delta t$ and could be used to estimate two-way travel time as well. However, symmetric events on the autocorrelation record tend to appear in a zone with small amplitudes due to the factor $(s^2 - s_0^2)$, especially when calibration scalar s is close to the correct value (Figures 2b and 2c). In contrast, antisymmetric events on the cross-correlation record have high amplitude since the zero-phase part of the sum is multiplied by the factor $(1 - Z^*Z)$ (Figure 3). This fact makes the cross-correlation record more robust for estimation of Δt.

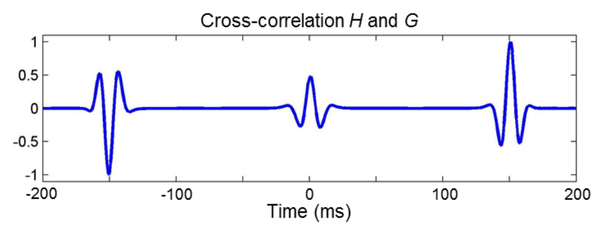

Figure 3: Cross-correlation of geophone and hydrophone zero-offset traces. Note anti-symmetric events with large amplitudes compared to event at t = 0 ms.

To sum up, the algorithm for estimation of the calibration scalar consists of the following steps:

- computing the cross-correlation of the geophone and hydrophone reflection data with muted direct arrivals;
- estimating the two-way travel time ($2\Delta t$) based on location of antisymmetric events on the correlation results; for buried receiver it can be estimated directly from first break time;
- varying s values and computing autocorrelations of $(H + sG)$;
- picking the s value which minimizes amplitudes of the autocorrelation around time $t = 2\Delta t$.

Application to a complex model

In this section we demonstrate application of our method to a complex synthetic model aimed at replicating a buried receiver acquisition in Saudi Arabia Bakulin et al. (2012). To compute the wavefield we use 2D finite-difference code and the velocity model shown in Figure 4. The wavefield is generated using a vertical force source with 50 Hz dominant frequency placed at the free surface. Geophone and hydrophone are buried at 30 m depth. The presence of thin layers with high contrast, along

DOI http://dx.doi.org/10.1190/segam2014-1082.1

with the free surface introduces numerous reflections, internal and free surface multiples (Figures 4a and 4b). A study on wave propagation in this model was conducted in our previous work (Alexandrov et al., 2012).

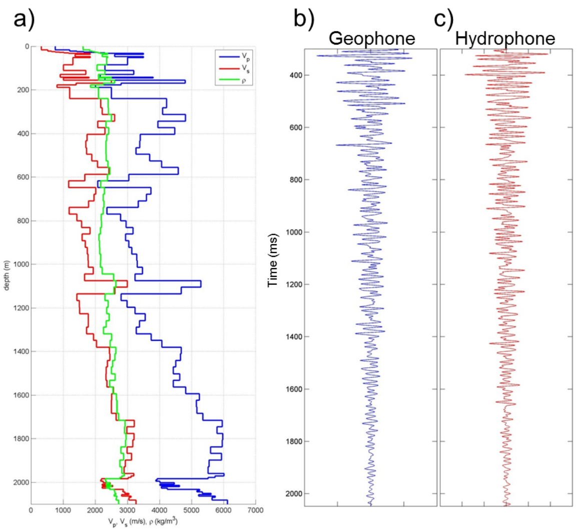

Figure 4: Velocity model used for synthetic modeling (a) and zero-offset traces recorded by geophone (a) and hydrophone (b).

First we perform an initial basic scaling of the geophone. The scaling assumes that the first arrival on the seismogram (Figure 5) contains only the direct downgoing wave and therefore the geophone is normalized to have the same first arrival amplitude as the hydrophone (although having opposite polarity) (Figure 5). After this initial scaling, the range of variation in scalar is reduced and s_0 should be close to unity.

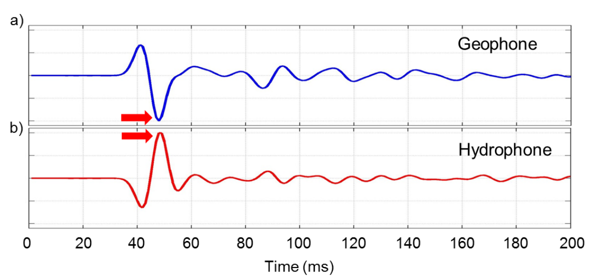

Figure 5: Early arrivals on zero-offset traces recorded by geophone (a) and hydrophone (b). Arrows indicate oppositie polarity amplitudes used to derive initial scalar.

Following the workflow described above, we start with estimation of the two-way travel time from the receiver depth to the free surface, which for this model is equal to 62 ms. This estimate is easily obtainable from picking first-breaks time on the buried receiver data. To perform the next step we mute the first 300 ms of geophone and hydrophone records to remove the direct wave and cross-correlate these traces. Then we choose a

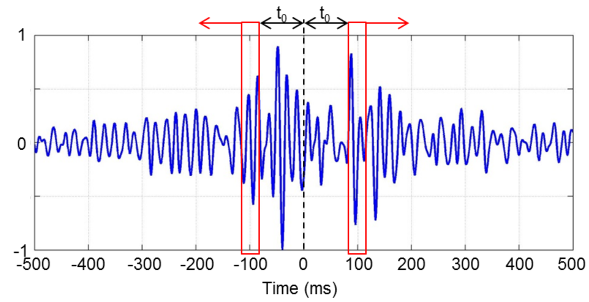

Figure 6: Cross-correlation of geophone and hydrophone zero-offset traces. Red squres indicate the two time gates where we are looking for antisymmetric events.

pair of time windows of the same length placed symmetrically with respect to zero time (Figure 6). We calculate the normalized root mean square (NRMS) difference between a part of the cross-correlation in one time window and a part in another time window multiplied by -1. We shift the time windows simultaneously away from time $t = 0$ and obtain dependence of NRMS difference on starting location of the time window t_0 (Figure 7). Clearly, minima on this graph correspond to the locations of antisymmetric segments of the cross-correlation. Due to complexity of the model NRMS never reaches zero because primary reflection arrivals and reflection ghosts are obscured by internal and free surface multiples. This interference leads to the appearance of extra minima which are not necessarily related to the ghost arrivals. As a result, in addition to the correct minimum location at 65 ms, we observe two more at 256 ms and 440 ms (Figure 7). In cases like this some additional information should be used to choose the correct minima. For instance, first breaks can be a good estimate of the one-way travel time for buried receiver acquisition or streamer depth divided by water velocity for marine case. Once we have estimated the two-way travel time t_0 we

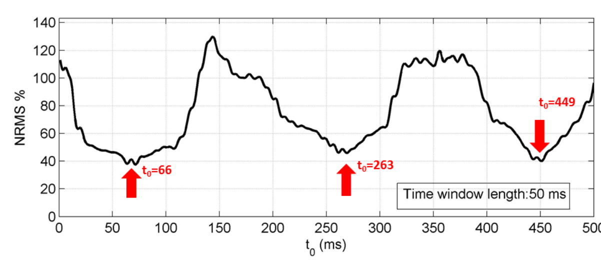

Figure 7: NRMS between part of geophone and hydrophone cross-correlation inside the window at t_0 and inverted cross-correltaion inside the window at $-t_0$, computed with 50 ms time gate length.

proceed to the next step and compute the autocorrelation of the sum $H + sG$ with a trial parameter s. We then vary s between 0.05 and 20 and use the stacked amplitude of squared autocorrelation inside the window placed at t_0 as a measure of the energy we want to minimize. The results are shown in Figure 8 for different lengths of the time gate. For display purposes, we apply a logarithmic scale to the x-axis. After the elementary

DOI http://dx.doi.org/10.1190/segam2014-1082.1

scaling we performed in the beginning, the theoretical value of s_0, computed from the acoustic impedance (Wapenaar, 1998), is equal to 1.71. This is indicated with a vertical dashed line at $\ln(s) = 0.53$. With the time gate of 40 ms length we obtain an energy minimum at the expected theoretical value of the scalar (Figure 8a).

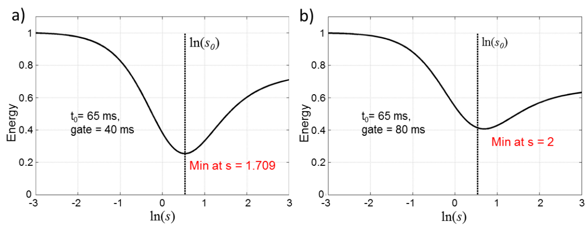

Figure 8: Energy of $H + sG$ autocorrelation computed for different values of calibration scalar s inside a time window centered around 65 ms with length of 40 ms (a), and 80 ms (b). Theoretical value of calibration scalar s_0 is indicated with a vertical dashed line.

Discussion

The NRMS value in Figure 7 was obtained with the specific size of the time gate chosen for comparison of the cross-correlation segments. The gate length depends on frequency of the signal. Because we are using a 50 Hz Ricker wavelet in the modeling, the cross-correlation of the two single arrivals is about 40-50 ms in length. If we use a smaller time window the NRMS values becomes less stable and start oscillating. This makes it less reliable for picking the correct minima. Longer time gates allow us to take into account several reflections, which may arrive one after another, and their ghosts. However, the greater the amount of interference from reflection arrivals and multiples the less pronounced the NRMS minima will be.

We use the same reasoning to choose a time gate for obtaining the energy graph shown in Figure 8. When we use a gate two times longer than that necessary to fit in the signal, the energy minimum shifts to the value $s = 2$, which is almost 20% greater than the correct one (Figure 8b). Nevertheless, dual sensor summation with this value of calibration scalar shows results similar to summation with the correct calibration (Figure 8c-f), suggesting that sensitivity of the separated wavefield to the value of the scalar is not strong.

Estimation of the two-way travel time from the analysis of cross-correlation of geophone and hydrophone in complex models can be ambiguous. Numerous internal reflections may lead to additional minima on the NRMS graph (Figure 7). If we use incorrect values of t_0 in further analysis the energy of $H + sG$ autocorrelation may have a minimum in the wrong location or have no minimum at all. In such cases, picking two-way travel time values should be done based on a priori information.

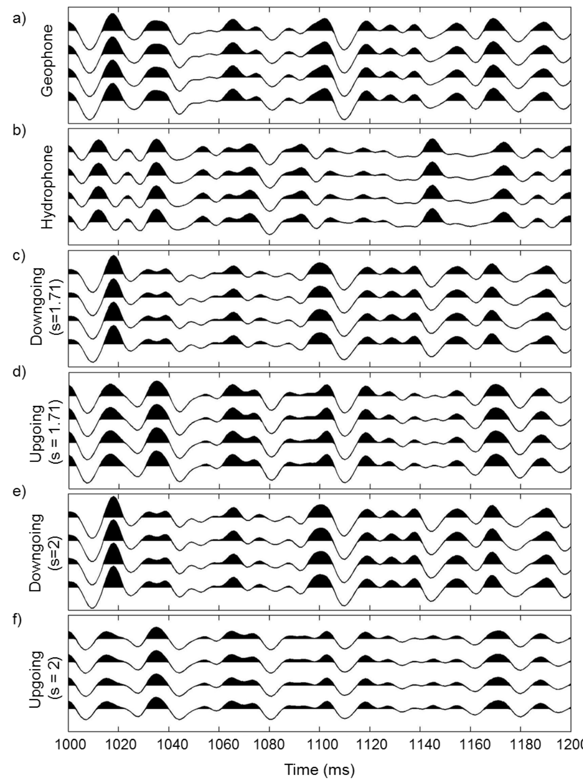

Figure 9: A segment of zero-offset traces for: full geophone (a), full hydrophone (b), downgoing (c) and upgoing (d) wavefield after summation with $s = 1.71$, downgoing (e) and upgoing (f) wavefield after summation with $s = 2$.

Conclusions

We presented a method to find a geophone scalar for dual-sensor summation and demonstrated efficiency of this technique in a complex media. To estimate calibration factors, we minimized a specific time window of the autocorrelation of the summed geophone and hydrophone pairs. Such an approach does not require knowledge of the velocity model. However, the position of the time window proved to be very important for correct calibration. This position is governed by the two-way travel time from the receiver level to the surface and can be found from analysis of geophone and hydrophone cross-correlation minima. Multiple internal reflections in models with a large number of layers can create additional minima on the cross-correlation. These extra minima can be mistakenly identified as those related to the two-way travel time. Therefore, in practice a priori information about zero-offset times from buried receivers will be highly beneficial.

Acknowledgments

We would like to thank Saudi Aramco for allowing us to publish this work.

http://dx.doi.org/10.1190/segam2014-1082.1

EDITED REFERENCES

Note: This reference list is a copy-edited version of the reference list submitted by the author. Reference lists for the 2014 SEG Technical Program Expanded Abstracts have been copy edited so that references provided with the online metadata for each paper will achieve a high degree of linking to cited sources that appear on the Web.

REFERENCES

Alexandrov, D., A. Bakulin, and R. Burnstad, 2012, Redatuming of synthetic land data with shallow buried receivers using the virtual source method: 82nd Annual International Meeting, SEG, Expanded Abstracts, doi:10.1190/segam2012-0295.1.

Bakulin, A., R. Burnstad, M. Jervis, and P. Kelamis, 2012, The feasibility of permanent land seismic monitoring with buried geophones and hydrophones in a desert environment: 74th Annual International Conference and Exhibition, EAGE, Extended Abstracts, X038.

Barr, F. J., 1997, Dual-sensor OBC technology: The Leading Edge, **16**, 45–52, http://dx.doi.org/10.1190/1.1437427.

Burnstad, R., A. Bakulin, M. Jervis, and D. Alexandrov, 2012, Successful imaging of land hydrophone and dual sensor data in a dry desert environment: 82nd Annual International Meeting, SEG, Expanded Abstracts, doi:10.1190/segam2012-0957.1.

Dragoset, B., and F. Barr, 1994, Ocean-bottom cable dual-sensor scaling: 64th Annual International Meeting, SEG, Expanded Abstracts, 857–860.

Soubaras, R., 1996, Ocean bottom hydrophone and geophone processing: 66th Annual International Meeting, SEG, Expanded Abstracts, 24–27, doi: 10.1190/1.1826611.

Wapenaar, K., 1998, Reciprocity properties of one-way propagators: Geophysics, **63**, 1795–1798, http://dx.doi.org/10.1190/1.1444473.